B. Urgošík

Effects of the axial component of the space charge electric field in the omegatron

Terms of use:

Effects of the Axial Component of the Space Charge Electric Field in the Omegatron

B. URGOŠÍK

Departement of Electronics and Vacuum Physics, Charles University, Prague*)

The axial component of the electric field generated by the space charge of the electron beam in omegatron causes a drift of trajectories of resonant ions in axial direction. Depending on working conditions, this drift leads to focusation or defocusation of resonant ions on the collector. Under certain conditions only ions generated in certain regions of the electron beam can reach the collector. The sum of these regions represents the effective length of the electron beam. The effective length starts with a value corresponding to the width of the collector, has an increasing part (region of focusation), a constant part equal to the geometric length of the beam and a steep decreasing part (region of defocusation). The analytic form for the effective length is derived at very simplified assumptions, still the comparison with experiments gives a good correspondence.

Влияние осевой составляющей электрического поля пространственного заряда электронов в омегатрону. — Благодаря осевой составляющей электрического поля пространственного заряда электронного пучка в омегатрону получают ионы аксияльный импульс, и в следствие того движутся тоже вдоль оси системы. В зависимости от условий работы приводит этот дрифт к фокусировке или дефокусировке ионов на колектор. Сумма областей пучка, из которых ионы могут попасть на колектор, представляет эффективную длину пучка. В работе приводится аналитическое выражение эффективной длины; хотя оно было получено за щет урощений, получается хороший соглас между теорией и экспериментом.

Účinky osové složky elektrického pole prostorového náboje elektronů v omegatronu. Osová složka elektrického pole prostorového náboje elektronového svazku v omegatronu způsobuje drift trajektorie rezonančního iontu v axiálním směru. V závislosti na pracovních podmínkách může tento drift vést k fokuzaci nebo defokuzaci rezonančních iontů na kolektor. Součet oblastí svazku, z nichž mohou ionty dopadnout na kolektor, představují účinnou délku svazku. V práci je odvozen analytický tvar účinné délky za velmi zjednodušených podmínek, avšak porovnání s experimenty vede přesto k dobrému souhlasu.

I. Introduction

In paper [1] a set of experimental characteristics of the omegatron is given. Analysis of the results shows that the influence of the electron beam cannot be restricted to ionization only. Especially the non-linear dependence of the resonant ion current

---

*) 121 16 Praha 2, Ke Karlovu 5, Czechoslovakia

on the electron current and a certain irregularity in the dependence of the ion current on the rf voltage cannot be accounted for without considering the space charge of the electron beam.

Space charge effects caused by the radial electric field component of the electron beam are treated in detail in [2]. In the present paper effects of the axial component of space charge electric field are explained.

As the potential minimum is situated at the middle length of the electron beam, the intensity of the space charge electric field is directed from the ends to the centre of the electron beam. This electric field accelerates the ions and their trajectories drift in the corresponding direction. Under certain conditions resonant ions from the axial boundaries of the electron beam can be focused on the collector, but also resonant ions originated in the region bellow the collector can be defocused. In general, it can be stated that the axial electric field can strongly influence the collection of resonant ions.

Although these space charge effects can be clearly understood in qualitative sense, the quantitative evaluation requires a rather sophisticated mathematical treatment. In order to get results which would be easy to survey we decided to introduce from the beginning some very serious simplifications. Although our model of the space charge effects on resonant ions is strongly simplified, it is still able to get into context all important parameters which determine the working conditions of the omegatron including the geometry.

In the socond part of this paper theoretical results are compared with experimental data. Experiments quoted here are treated in detail in [1]. Experimental results are in good qualitative agreement with the theory, in some special cases even a quantitative correspondence is obtained.

2. Estimate of the Axial Component of the Electric Field

The potential distribution on the axis of a cylindrical electron beam is of a rather complicated course and can be approximated e.g. by a Fourier series with Bessel coefficients [3]. Such a complicated potential is useless for our task to find and approximate though adequately simple expression for the potential distribution which would enable to linearize the equations of motion of the ion.

Let us consider a cylindrical electron beam of radius a, length L and current density j, placed in a cylindrical coordinate system the axis z of which corresponds to the axis of the beam (Fig. 1). Let us assume the same accelerating potential V_0 at both ends of the beam. The potential distribution $\Phi(z)$ on the axis can be approximated by

$$\Phi(z) = V_0 - \frac{A}{2}\frac{L^2}{4} + \frac{A}{2}z^2, \qquad (1)$$

where

$$A = \chi \frac{j}{\varepsilon_0 \sqrt{2\eta V_0}}, \qquad A > 0,$$

20

and η is the charge-to-mass ratio of the electron and ε_0 the permitivity. The quality χ is introduced as a factor correcting the error of the method. Comparing results obtained by means of (1) with those obtained with the aid of a more correct
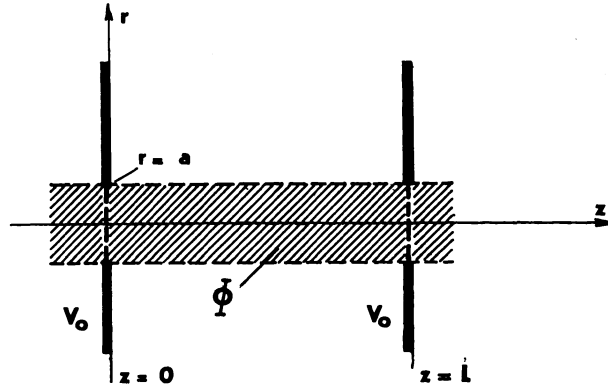

Fig. 1.

function (e.g. in [3]) χ can be estimated at conditions currently used in the omegatron ($L \sim 2$ cm, $a \sim 0.5$ mm, $i \sim 10$ µA) to be

$$\chi = 5 \times 10^{-3}.$$

The axial component of the electric field from the space charge is then

$$\mathscr{E} = -\frac{d\Phi}{dz} = -Az \tag{2}$$

The potential distribution given by (1) and the electric field given by (2) is unprecise not only due to violation of the Poisson equation, but it also does not take into account the distortion caused by the anode and the cathode apertures and the presence of positive ions in the beam. On the other hand, formula (2) gives a linear equation of motion.

Taking the electron current i in µA, we obtain with $a = 5 \times 10^{-4}$ m, $L = 2 \times 10^{-2}$ m and $V_0 = 100$ V

$$A \approx 1.2 \times 10^2 \, i.$$

The potential depression being according to (1)

$$-\frac{A L^2}{8},$$

its value e.g. for $i = 10$ µA is -58 mV. For the same current the field of the boundary of the electron beam ($z = 1 \times 10^{-2}$ m) is $\mathscr{E} = 12$ Vm^{-1}. This value is of the same order as the amplitude of the rf electric field at rf voltage of about 1 V.

3. Equations of motion

Let us find the perturbation of the trajectory of a resonant ion caused by the axial electric field in the electron beam.

Before making up the equations of motion it is necessary to make some assumptions concerning the distance of action of the axial field. The resonant ion will move off the axis in the radial direction while formula (2) is valid only at the axis, i.e. for $r = 0$. For this reason we must introduce another approximate assumption: suppose (2) is valid within the whole electron beam, while outside $\mathscr{E} = 0$ holds. This means that the force excercised by the sapce charge field on an ion of the charge $+ e$ is

$$- eAz$$

for $- L/2 \leq z \leq L/2$ and $0 \leq r \leq a$; outside this region the force is zero.

An ion in the omegatron will move under the influence of three fields: the static space-charge field, the external rf electric field $E \sin \omega t$ and the external magnetic field B. External fields are supposed to be homogeneous and perpendicular to each
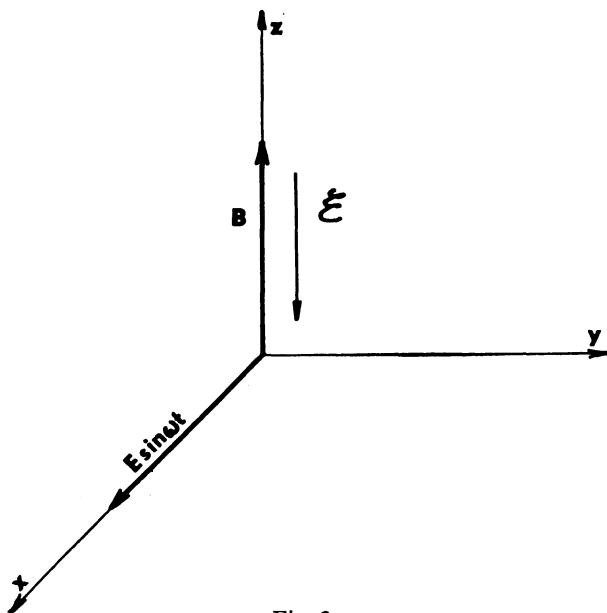

Fig. 2.

other. Let us introduce a Cartesian system xyz such that the z axis corresponds to the axis of the electron beam and the origin is situated at the middle length of the electron beam. The rf electric field lies in the x axis and the magnetic field in the positive z axis (Fig. 2). In this system the axial component of the space charge field is directed opposite to the z axis.

The equations of motion for an ion with specific charge e/m generated inside the electron beam have the form:

$$\ddot{x} = \alpha \sin \omega t + \dot{y}\omega_c, \tag{3a}$$

$$\ddot{y} = - \dot{x}\,\omega_c, \tag{3b}$$

$$\ddot{z} = - \varepsilon^2 z, \tag{3c}$$

where

$$\alpha = \frac{eE}{m}, \tag{4a}$$

$$\omega_c = \frac{eB}{m}, \tag{4b}$$

$$\varepsilon^2 = \frac{eA}{m} \tag{4c}$$

Formula (4b) gives the angular cyclotrone frequency of an ion and since we consider the case of resonance, $\omega_c = \omega$.

Equations (3) can be separated into two parts. The first two equations represent a system of mutually dependent differential equations, while the third one can be solved independently, the solution being:

$$z = C \cos (\varepsilon t_1 + \psi).$$

By notation t_1 we emphasize that its validity is limited to the time interval before the ion has left the electron beam. With the initial conditions $z = Z$ and $\dot{z} = 0$ for $t_1 = 0$ we have $C = Z$ and $\psi = 0$, which leads to

$$z = Z \cos \varepsilon t_1, \tag{5}$$

$$\dot{z} = - \varepsilon Z \sin \varepsilon t_1 \tag{6}$$

The system (3a), (3b) was solved by Berry [4] as a two-dimensional problem. It follows from his solution that the trajectory of a resonant ion generated at the origin, when disregarding the initial velocity and the initial phase of the rf field, can be approximated by a spiral of Archimedes. In complex notation the approximate trajectory takes the form:

$$x + iy \doteq - \frac{\alpha}{2\omega} e^{-i\omega t} \tag{7}$$

It is quite appropriate when taking the trajectory as a whole (i.e. from its origin to the collector), but it is dubious when considering the motion of an ion near the origin, which means within the electron beam. On the other hand, our estimate of the axial space charge field is very rough and it would not be purposeful to combine an approximate equation (5) with a strict solution of (3a) and (3b). For this reason, in our model, equation (7) holds within the electron beam, as well.

23

Equation (7) was derived for an ion generated at the origin of the coordinate system, but the fields being homogeneous it is valid for any point of generation on the z axis. It remains to consider the ions created off this axis. This is easy as the applied fields are homogeneous and the approximate trajectory is again a spiral of Archimedes its origin being situated at the point of generation of the considered ion. It is more difficult to consider the influence of the axial space charge field on the resulting trajectory $x(t), y(t), z(t)$. The ion in dependence on the point of generation and on the ratio of the spiral pace to the radius of the electron beam can leave and enter the electron beam several times, before getting out of it. This complicates the evaluation of the resulting axial velocity of the ion when leaving the electron beam. Still more difficulties will be met in the following procedure when selecting those regions in the electron beam from which the ions will not be able to reach the collector. It can be demonstrated that these regions are limited by transcendents with harmonic singularities.

With the aim to arrive at final results in a concise form we abstain from a general solution of the problem and introduce the last simplification assuming that the ions are generated only on the z axis and that (7) holds for all resonant ions.

Expressing (7) in polar coordinateds r, φ it becomes

$$r = \frac{\alpha t}{2\omega}$$

$$\varphi = \omega t \tag{8}$$

Inserting for α and ω from (4a) and (4b) we get

$$r = \frac{Et}{2B} \tag{9}$$

The resulting trajectory of a resonant ion is a superposition of motion described by (5), (8) and (9). In radial direction an ion will move off the z axis with a constant velocity $E/2B$ and rotate about the same axis with a constant angular velocity ω and it will drift in the axial direction. While inside the electron beam the axial velocity is given by (6), after leaving the beam of radius a the axial velocity will be constant and equal to

$$\dot{z} = - \varepsilon Z \sin \varepsilon \tau$$

where $\tau = t_1$ for $r = a$. Inserting from (9) we get

$$\tau = 2a \frac{B}{E} \tag{10}$$

An ion that originated exactly at the middle length of the electron beam $(Z = 0)$, or reached the boundary of the beam exactly after a time given by $\varepsilon \tau = n\pi$ leaves the beam with zero axial velocity. The trajectory in this case is a pure spiral of Archimedes.

4. Circles of Focusation

Let us separtae the axial coordinate of the ion trajectory into two parts

$$z = z_1 + z_2$$

where z_1 is the coordinate at the moment when the ion leaves the electron beam and z_2 the coordinate after the ion has left the beam. According to this notation

$$z_1 = Z \cos \varepsilon \tau \,,$$
$$z_2 = t_2 (\dot{z})_\tau = - t_2 \varepsilon \, Z \sin \varepsilon \tau \,, \tag{11}$$

where $t_2 = 0$ when the ion leaves the beam. For $r \geqslant a$ the radial position of an ion corresponding to z_2 according to (9) is given by

$$r - a = \frac{E}{2B} t_2 \,,$$

whence

$$t_2 = (r - a) \frac{2B}{E}$$

and

$$z_2 = - (r - a) \frac{2B}{E} \varepsilon Z \sin \varepsilon \tau$$

Considering (11) we get

$$z = Z \left[\cos \varepsilon \tau - 2\varepsilon(r - a) \frac{2B}{E} \sin \varepsilon \tau \right] \tag{12}$$

which is valid for $r \geqslant a$, the parameter being r.

Equation (12) is not the trajectory of an ion, as it gives no information about the φ coordinate. Imagine for a moment that (12) be the solution of a certain problem with rotational symmetry in r, z. It describes a surface consisting of a frustum of cone of height $(z_2 - z_1)$ and a rotational symmetric surface of height z_1 (Fig. 3). The trajectory of a resonant ion in this case represents a spiral curve wound on the frustum of a cone.

The angular position of the ion is uninteresting for our purpose until the moment when the ion reaches the collector. The geometry requires to consider the whole problem in rotational symmetry. In this case it is necessary to replace the collector by a cylinder of the same radius R. The only error thus introduced consists in a different radius r when the ion reaches the fictive collector and the real one. This error equals at most the increase of r for one spiral orbit. Considering that the ion must perform 10 to 100 orbital motions before reaching the collector it is negligible.

In a rotational symmetry so introduce the spiral wound on the cone is replaced by this "basic" cone itself. Every meridional intersection of the "basic" cone can be taken for a "ray" of the ion and (12) represents the equation of this "ray".

Let us seek the radii $r = f$ of basic cones of ions generated at various points Z of the z axis (Z variable) at their passing the position $z = 0$. It follows from (12):

$$0 = Z\left[\cos \varepsilon\tau - 2\varepsilon\,(f - a)\,\frac{B}{E}\,\sin \varepsilon\tau\right]$$

For

$$Z \neq 0 \quad \text{and} \quad \varepsilon\tau \neq n\pi, \qquad n = 0, 1, 2, \ldots$$

we get

$$f = a + \frac{E}{2\varepsilon B}\,\cot \varepsilon\tau \tag{13}$$

After inserting for ε and τ from (4c) and (10) we get also

$$f = a + \frac{E}{2B\sqrt{\dfrac{e}{m}\,A}}\,\cot\left(\sqrt{\dfrac{e}{m}\,A \cdot 2a\,\dfrac{B}{E}}\right)$$
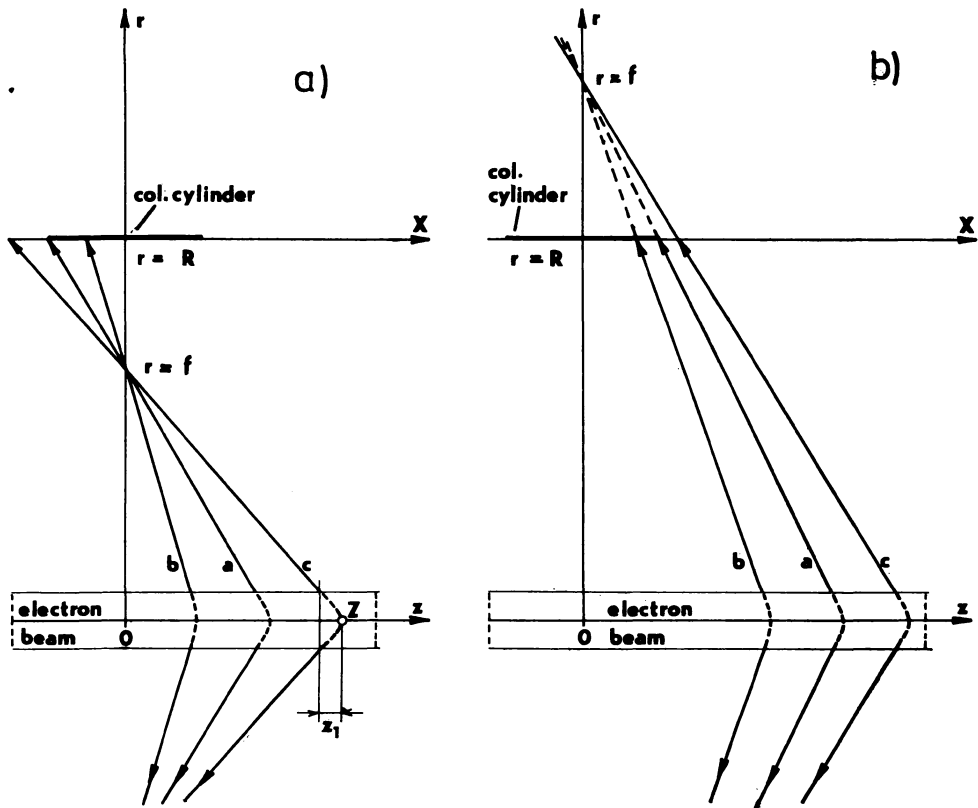

Fig. 3.

These relations are valid for all ions excluding those that left the beam with zero axial velocity.

It is clear that with the exception of some singularities the radius f does not depend on the point of generation of the ion and, with the same working coditions (E, B, A), it is identical for all ions with the same charge-to-mass ratio. The "rays" of all ions with the same e/m intersect and the points of intersection lie on a circle of radius f. It can be denoted as the circle of focusation.

By the existence of the circles of focusation the influence of the axial electric field generated by the space charge of the elecgtron beam on collection of ions can be accounted for in a plausibile way. Fig. 3 represents two radii f in relation to the radial position R of the collector cylinder. In Fig. 3a the circle of focusation lies below the collector, in Fig. 3b above it. In both cases the rays a represent the limiting rays which strike the boundaries of the collector, rays b are inner rays and c are outer rays. It can be seen that in both cases only ions situated within the region enclosed by the limiting rays can reach the collector. In the first case a decrease of f causes narrowing of the inner region, in the second case its broadening. It is remarcable that f depends on A, which is proportional to the electron current i.

5. The Imaging Equation

Suppose an infinite cylinder of radius R in cylindrical coordinates with the z axis corresponding to the axis of the cylinder. Let us denote one of the straight lines of the meridional section X and let us take it for a parameter. Its origin $X = 0$ corresponds to $z = 0$ shifted in the distance R. The collector cylinder is a part of this infinite cylinder the bases of which are placed at $X = D/2$ and $X = -D/2$, D being the length of the collector (Fig. 3).

The line of intersection of the basic cone with the infinite cylinder, the point of intersection of the ion "ray" with the X-line resp. can be obtained from the condition

$$X = z \Big|_{r = R} , \tag{14}$$

where z is given by (12).

Before inserting (14) into (12) let us introduce the following notation:

$$\beta = \frac{2B}{E}$$

$$P = R - a , \tag{15}$$

$$\varkappa = \varepsilon \beta \tag{16}$$

According to it $\tau = \beta a$ and

$$\varepsilon \tau = \varkappa a \tag{17}$$

Inserting (14), (16) and (17) into (12) we get

$$X = Z(\cos \varkappa a - \varkappa P \sin \varkappa a) \tag{18}$$

27

This equation gives information how to image any point from the axis z of the electron beam through the ion "rays" onto the infinite cylinder a part of which is the collector. The values of the external fields and of the space charge field are comprised in just one parameter $\varkappa$, the rest being only parameters of geometry. This is significant.

Let us now seek those points on the z axis, which are imaged just onto the edges of the collector. The left edge will be struck by ions generated at Z which satisfieds the imaging equation (18) for $X = - D/2$, i.e.

$$- \frac{D}{2} = Z(\cos \varkappa a - \varkappa P \sin \varkappa a) \,.$$

Expressing Z we get

$$Z^- = - \frac{1}{2} \frac{D}{\cos \varkappa a - \varkappa P \sin \varkappa a} \tag{19}$$

(by the symbol Z^- it is emphasized that the equation holds for the left edge of the collector). For the right edge $(X = D/2)$ we get

$$Z^+ = \frac{1}{2} \frac{D}{\cos \varkappa a - \varkappa P \sin \varkappa a} \tag{20}$$

The curves (19) and (20) are symmetrical in respect to the z axis (Fig. 4) and with singularities at

$$\cos \varkappa a = \varkappa P \sin \varkappa a$$

i.e. for

$$P = \frac{1}{\varkappa} \cot \varkappa a \,. \tag{21}$$

Comparing this equation with (13) gives a singularity for $f = R$, i.e. in the case when the circle of focusation just reaches the collector cylinder. Naturally, when all the ions strike the centre of the collector no one can reach the edges.

The singularities are periodical according to the π — periode of the function cot. It follows that the lines Z^- and Z^+ desintegrate into several sections: at the first singularity into two sections, at the second into three sections etc. We shall denote these sections by indices: before the first singularity with 1 (Z_1^+, Z_1^-), after the first singularity with 2 (Z_2^+, Z_2^-) etc. With a given geometry (P, D, a) the curves of limit imaging are functions of the parameter $\varkappa$ only. In the following we shall demonstrate that for values $\varkappa$ only the first singularity has to be considered in all practical cases.

The curves of limit imaging are in Fig. 4 (in arbitrary scale). For $\varkappa = 0$ $Z^+ = D/2$, $Z^- = - D/2$, which means that the edge of the collector chosen is reached by ions coming from the points on the axis situated close under the edge of

28

the collector. This corresponds to $f \to \infty$. With $\varkappa$ increasing the ions will reach the edge arriving from a region shifted to the corresplonding boundary of the electron beam. This corresponds to $f > R$, but f finite. At a certain value of $\varkappa$, $\varkappa = \varkappa_1$, the curves of limit imaging reach exactly the values $\pm L/2$. This corresponds to the
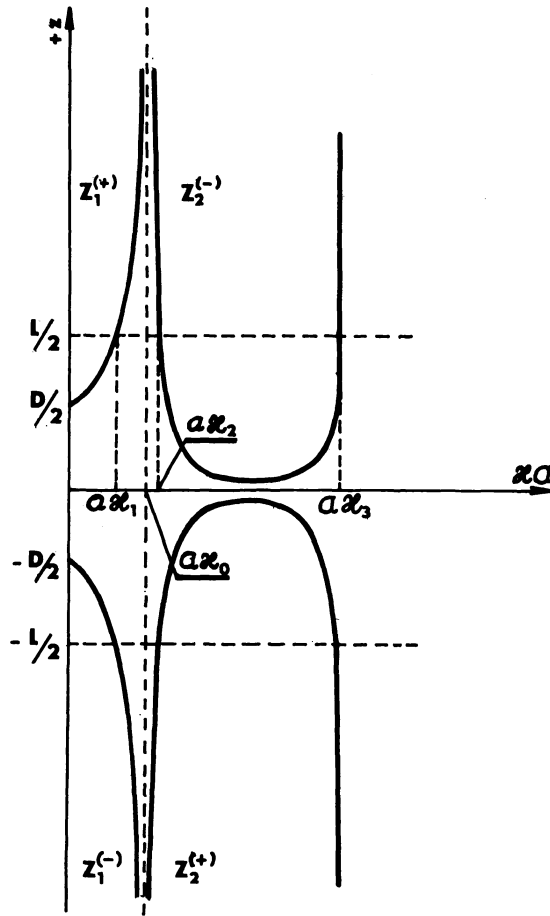

Fig. 4.

situation when the right edge of the collector is reached by the ions from the boundary of the right half-beam and vice versa. Increasing above this value causes the singularity ($\varkappa = \varkappa_0$) and then the values Z^+ and Z^- change the signs. At $\varkappa = \varkappa_2$ the left edge of the collector is reached by ions generated at the boundary of the right half-beam and vice versa. This situation is repeated for $\varkappa = \varkappa_3$. From the analysis of the curves of limit imaging it is clear that because of a finite length L of the electron beam the singularities are "cut off".

29

6. Effective Length of the Beam

Inside the electron beam there are regions from where the ions cannot reach the collector and regions from where the ions are focused on the collector. The set of the latter ones will be denoted the effective length of the electron beam.

Assuming that only the first singularity occurs the collector cylinder will be reached by ions from all those regions of the beam whose coordinate Z of the point of generation fulfils the trivial condition

$$-\frac{L}{2} \le Z \le \frac{L}{2} \,,$$

and the additional conditions:

in the left half-beam	in the right half-beam
$Z_1^- \le Z \le 0$	$0 \le Z \le Z_1^+$
$Z_2^+ \le Z \le 0$	$0 \le Z \le Z_2^-$

The effective length S as a function of the parameter $\varkappa$ can be written as

$$S(\varkappa) \begin{cases} |Z_1^+| + |Z_1^-| & \text{for} \quad 0 \le \varkappa \le \varkappa_1 \,, \\ L & \text{for} \quad \varkappa_1 \le \varkappa \le \varkappa_2 \,, \\ |Z_2^+| + |Z_2^-| & \text{for} \quad \varkappa_2 \le \varkappa \le \varkappa_3 \,, \end{cases}$$

Because $|Z^+| = |Z^-|$ and because Z_1^+ and Z_2^+ do not differ in the analytic form, differing only in the domain of definition, taking into account (20), the above relation becomes

$$S \begin{cases} \left| \dfrac{D}{\cos \varkappa a - \varkappa P \sin \varkappa a} \right| & \text{for} \quad 0 \le \varkappa \le \varkappa_1 \,; \quad \varkappa_2 \le \varkappa \le \varkappa_3 \\[2mm] L & \text{for} \quad \varkappa_1 \le \varkappa \le \varkappa_2 \,, \end{cases} \tag{22}$$

with

$$\varkappa = \frac{2B}{E} \sqrt{\frac{e}{m} A} \,, \tag{23}$$

quantity A being of linear dependence on the electron current i.

In Fig. 5 the dependence of the effective length S on $\varkappa$ is plotted for $L = = 1.4 \times 10^{-2}$ m, $D = 8 \times 10^{-3}$ m, $R = 9 \times 10^{-3}$ m and $a = 5 \times 10^{-4}$ m (i.e. $P = 8.5 \times 10^{-3}$ m). These values correspond to the omegatron used in [1]. The real length of the electron beam was 2 cm and this value was inserted to assess the quantity A, but for determination of S only a part of the electron beam was considered, which was not screened off by the guard rings, giving 1.4 cm.

The full line in Fig. 5 corresponds to (22). It has three important regions: increasing, constant and decreasing. For values of $\varkappa > 4 \times 10^3\,\mathrm{m^{-1}}$ equation (22) gives another increasing region. At low values of $\varkappa$ the effective length $S(\varkappa)$ is near
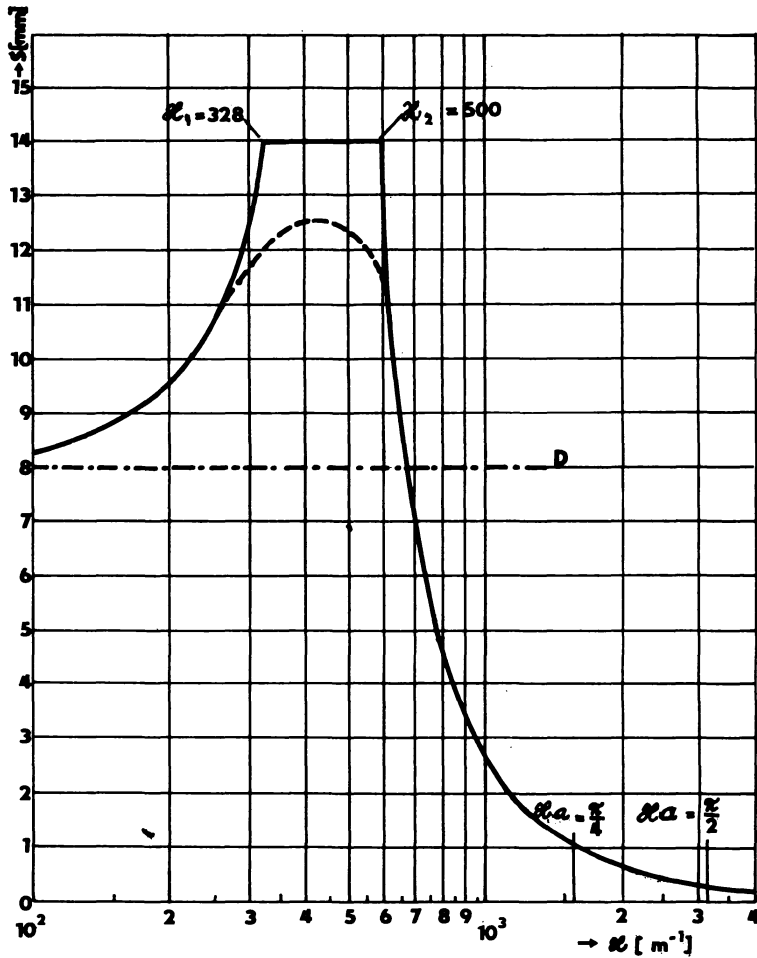

Fig. 5.

to the width of the collector D. With $\varkappa$ increasing (i.e. with i and B increasing or E and m decreasing) the ions are focused on the collector from the boundary regions of the beam and the effective length grows. The constant dependence corresponds to the interval $\varkappa_1 \leq \varkappa \leq \varkappa_2$ when the effective length reaches the full length of the beam. When the increase of $\varkappa$ consinues, a strong defocusing of ions takes place, the effective length falls sharply and in the vicinity of $\varkappa a = \pi/2$ it attains only a few percent of its maximum value.

31

The simplified model of collection, which introduces the effective length of the beam given by (22) works somewhat "hard". The estimates which take into account also the radial dependence of the point of generation of an ion in the beam show that the effective regions have not only an axial but also a radial structure. These estimates lead to the conclusion that it can never happen for ions of all the volume of the beam to be focused on the collector. The real effective length is always shorter than the geometric length and it attains about 90 % maximum. The dependence of the corrected effective length is plotted in Fig. 5 by dotted line.

7. Equation for the Current of Resonant Ions

Assuming no other losses of resonant ions than those caused by the influence of axial space charge electric field the current is given with the aid of a variable effective length (22) as

$$I = \sigma\, p_i\, S(\varkappa)\, i\,, \tag{24}$$

σ being the specific ionization and p_i the partial pressure of the considered gas.

It was demonstrated in [5] and [6] that losses of resonant ions are caused also by collisions with neutral molecules if the mean free path of molecules is of the same order as the trajectories of ions. In this case the ion current striking the collector can be expressed according to [6] as

$$I = I_0 \exp\left(-k\,\frac{eB^2R^2}{mE}\right)\,,$$

I_0 being the current that leaves the electron beam, k being a coeficient expressing losess and being proportional to the total gas pressure. This equation is valid under the assuption that no external constant voltage (e.g. trapping voltage) is applied.

Taking into account both collisions and axial space charge field, I_0 can be considered to be the current of ions reaching the collector if no collisions occur. Then inserting I_0 from (24) we can write

$$I = \sigma p_i S(\varkappa)\, i \exp\left[-k\,\frac{e}{m}\,\frac{B^2R^2d}{\sqrt{2}\,U}\right] \tag{25}$$

Instead of the intensity E of the radiofrequency field the voltage U and the distance d of the electrodes are used here. Formula (23) can be transformed accordingly into a practical form. For the omegatron which gave experimental results in [1] $A = = 1.2 \times 10^2\, i, d = 2 \times 10^{-2}$ m and

$$\varkappa \doteq 3.10^3 \sqrt{\frac{i}{M}}\,\frac{B}{U}\,,$$

M being the mass number of the ion considered.

It is convenient to introduce $\varkappa$ pertaining to the electron current 1 μA, or $\varkappa$ pertaining to rf voltage 1 V.

Let us denote:

$$\varkappa^\star = \varkappa \Big|_{i = 1\ \mu A} \, ; \qquad\qquad {}^\star\varkappa = \varkappa \Big|_{U = 1\ V} \, .$$
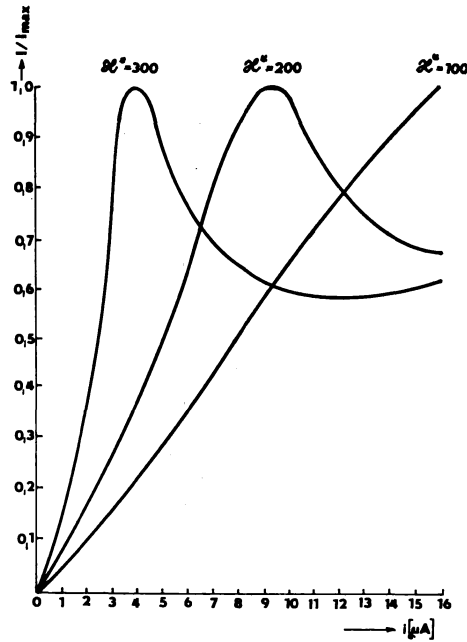

Fig. 6.

8. Comparison of the Theory With Experiments

A. Dependence of the ion current I on the electron current i:

$$I = I(i)$$

Edwards [7] demonstrated that the experimental characteristic $I = I(i)$ is not linear as it could be expected and that the deviation from linearity in dependence on working conditions was less or more expressed and sometimes went through maxima. The same qualitative result is obtained from (24) or (25).

In Fig. 6 theoretical reduced values of I/I_{max} are plotted in dependence on i according to (24). To determine S the corrected curve from Fig. 5 was used as it gives a better description of the physical nature of the effect. The plot shows clearly that for low values of $\varkappa^\star$ (low values of magnetic field B or higher values of rf voltage U) the theory gives a linear dependence. For higher values of $\varkappa^\star$ maxima

33

of various steepness can be formed, but as the curve for $\varkappa^\star = 300\ \text{m}^{-1}$ indicates even local minima can occur. The formation of minima has not been observed in experiments.
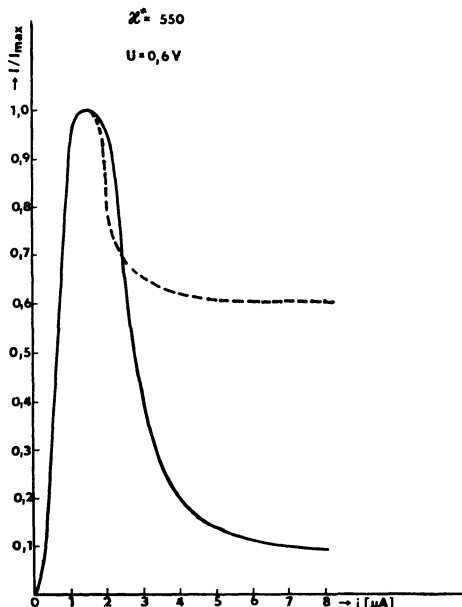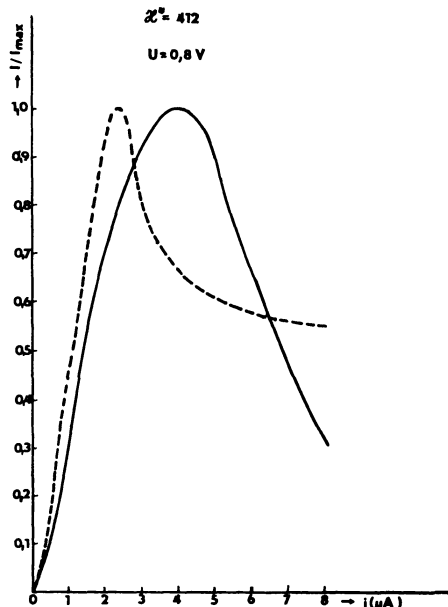

Fig. 7.

Fig. 8.

A quantitative comparison of theoretical and experimental values is plotted for four cases in figures 7–10. The dotted lines represent theoretical values, the full lines stand for experimental values from [1]. In figures 7 and 8 the values are for He^+ ions $(M = 4)$ at $B = 0.22\ \text{T}$ (trapping voltage $+ 0.2\ \text{V}$), in figures 9 and 10 for ions Ne^+ $(M = 20)$, $B = 0.3\ \text{T}$ (trapping voltage $+ 0.2\ \text{V}$). The characteristic in Fig. 7 was measured at the rf voltage $U = 0.6\ \text{V}$ which corresponds to $\varkappa^\star = 550\ \text{m}^{-1}$, the characteristic in Fig. 8 is for $U = 0.8\ \text{V}$ and $\varkappa^\star = 412\ \text{m}^{-1}$, in Fig. 9 $U = 1\ \text{V}$, $\varkappa^\star = 203\ \text{m}^{-1}$ and in Fig. 10 $U = 1.5\ \text{V}$ and $\varkappa^\star = 135\ \text{m}^{-1}$.

The theoretical and experimental reduced characteristics in Fig. 7 take an identical course from the beginning to the maximum, which takes place at the same value of $i = 1.5\ \mu\text{A}$, both curves differ in the decreasing parts. The agreement of the theory with the experiment is good. Unfortunately, with the rf voltage U increasing the discrepancy in theoretical and experimental curves for light ion increases.

For $U = 1\ \text{V}$ (Fig. 8) the agreement of characteristics is only qualitatively good, the theoretical maximum is shifted in comparison with the experimental curve to lower values electron current. For heavier ions of neon the positions of maximi are

inversed. At $U = 1.5$ V (Fig. 10) the quantitative agreement of the theoretical curve with the experimental one is good (I_{max} being the value of I at $i = 12$ μA). But at lower voltage $U = 1$ V (Fig. 9) the theory expects the characteristic with
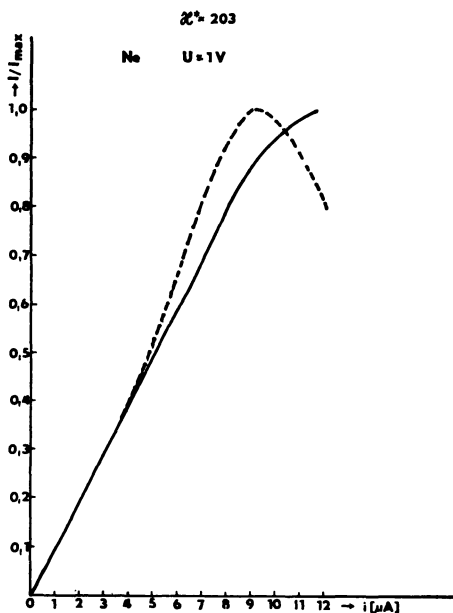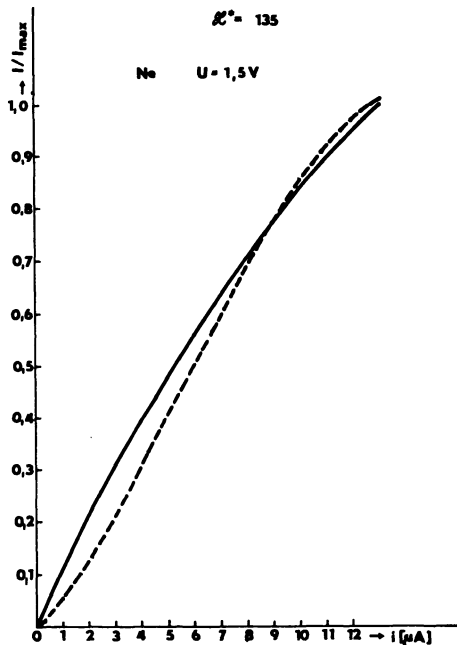

Fig. 9.

Fig. 10.

a maximum while the experimental curve up to electron currents $i = 12$ μA does not pass any maximum. At low electron currents (up to 5 μA) the agreement with the theory is still good.

B. Dependence of ion current on RF Voltage:

$$I = I(U)$$

The radiofrequency voltage U is contained in formula (25) twice: in the exponent (in connection with losses by collisions) and as argument of $\varkappa = \varkappa(U)$ while $\varkappa$ is a parameter of effective length S. We can introduce a new quantity G by

$$G = S(\varkappa(U)) \cdot e^{-\frac{\delta}{U}}, \qquad (26)$$

which expresses the integral effectivity of collection of resonant ions in dependence on U. Varying U only δ remains constant.

35

The plot of (26) for $^\star\varkappa = 100$ m^{-1} is in Fig. 11 for four different values of δ. The effective length was again determined by means of the corrected curve from Fig. 5. The curve for $\delta = 0$ is just a copy of a part of the curve from Fig. 5 in the opposi-
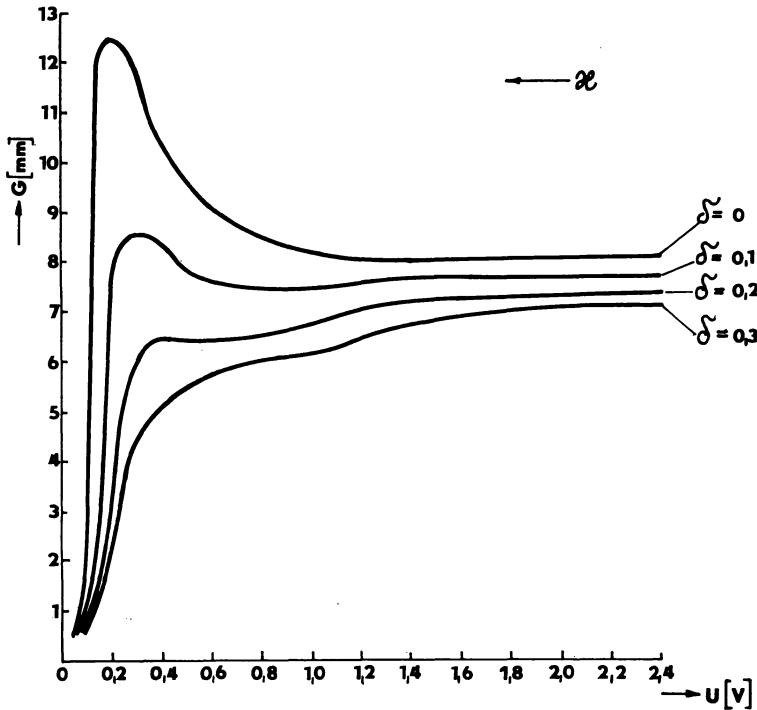

Fig. 11.

te sense. From the physical point of view all curves should start at $U = 0$, but the parameter $\varkappa$ diverges at this value, the curves of limit imaging go through an infinite number of singularities and the effective length S would theoreticaly reach its maximum values infinitely many times.

All the curves in Fig. 11 are very steep at low values of U, which agrees with the experiments. Curves for values of δ near zero show well expressed maxima, which disagrees with the experiments even when the measurements are performed at very low pressures, while the curves for $\delta \geqslant 0.2$ are quantitatively corresponding to the experimental characteristics $I = I(U)$ demonstrated in [1].

In Fig. 12 two measured characteristics $I = I(U)$ are given (full curves) according to [1]. They were measured for He$^+$ ions at the total pressure (and practically the same partial pressure) $p = p_{He} = 5.38 \times 10^{-4}$ Pa, at $B = 0.22$ T (and at trapping voltage $+ 0.1$ V) To compare these characteristics with the theory according to (25), the value of k or δ resp. in formula (26) must be found.

36

Let us choose at some measured characteristic $I = I(U)$ two points denoted 1 and 2. The following relations are valid:

$$I_1 = \sigma p_i i S_1 e^{-\frac{\delta}{U_1}} ,$$
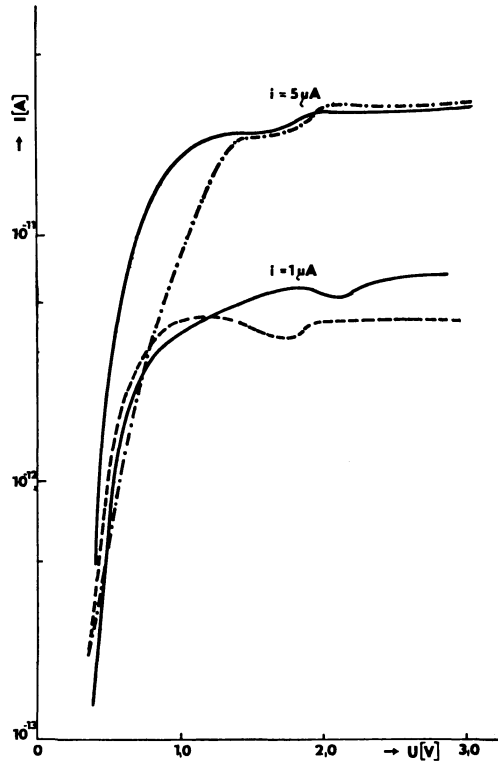
$$I_2 = \sigma p_i i S_2 e^{-\frac{\delta}{U_2}} ,$$

Fig. 12.

where
$$S_1 = S(\varkappa(U_1)), \qquad S_2 = S(\varkappa(U_2)) .$$

Whence

$$\delta = \frac{\lg \dfrac{I_1 S_2}{I_2 S_1}}{\dfrac{1}{U_2} - \dfrac{1}{U_1}} . \tag{27}$$

In order not to have too large an error when evaluating δ according to (27) it is necessary to find the conditions at which the theoretical and real effective lengths differ least. It is to be expected that the real and theoretical values of effective length

37

will be approaching the more, the lower the value of $\varkappa$, as for $\varkappa = 0$ (no axial forces), the theoretical as well as the real values of S are given only by the width D of the collector. The right-hand part of the characteristic for $i = 1 \, \mu\text{A}$ in Fig. 12 corresponds to low values of $\varkappa$.

Let us choose on the characteristic for $i = 1 \, \mu\text{A}$ (Fig. 12) $U_1 = 3 \, \text{V}$. Then $I_1 = 6.2 \times 10^{-12} \, \text{A}$ and evaluating $\varkappa$ gives $\varkappa_1 = 110 \, \text{m}^{-1}$ and finally $S_1 = = 8.35 \times 10^{-3} \, \text{m}$. In the same way choosing $U_2 = 2.6 \, \text{V}$ leads to $I_2 = 6.05 \times \times 10^{-12} \, \text{A}$, $\varkappa_2 = 126 \, \text{m}^{-1}$ and $S_2 = 8.5 \times 10^{-3} \, \text{m}$. Inserting these values into (27) we get $\delta \doteq 0.8$. The specific ionization of helium is $\sigma = 1.2 \, \text{Pa}^{-1} \, \text{m}^{-1}$ and the pressure in this case is $p_{He} = 5.33 \times 10^{-4} \, \text{Pa}$. Inserting the obtained values into (25) we get the theoretical characteristic for $i = 1 \, \mu\text{A}$ and $i = 5 \, \mu\text{A}$ represented in Fig. 12 by dotted lines.

At low electron currents ($i = 1 \, \mu\text{A}$) the correspondence of the theory with the experiments is very good in the region of low rf voltage. At the point $U = 1.1 \, \text{V}$ the two characteristics intersect and for higher voltages they differ. The correspondence in the sense of the order is still fairly good. More important is the fact that both characteristics attain local minima. In this way space charge effect of the axial component of the electric field helps to account for the nonuniformity of the characteristics measured.

At higher electron currents ($i = 5 \, \mu\text{A}$) the correspondence of the theory and the experiment starting from values of $U = 1.4 \, \text{V}$ is surprisingly good, while in the medium region of voltages (about 0.8 V) the differences amount to 70 %. With the voltage decreasing these differences decrease mildly.

Finally, it is to be stated that our theory does not consider the influence of the trapping voltage on the collection of ions, while all the experimental characteristics investigated here were measured (unfortunately) at a non-zero trapping voltage.

9. Conclusion

The model of influence of the electron beam on resonant ions is considerably simplified. The simplifications concern the value and the analytic form of the axial component of the space charge electric field, the extent of this field in radial direction, also the trajectories of ions in the plane perpendicular to the magnetic field are simplified and finally the time interval during which the ions stay under the influence of this field is approximated. Notwithstanding these simplifications all the measured dependences of the ion current on the electron current can be explained on the basis of our model, which is also true for the nonumiformity of the characteristics $I = I(U)$. In some cases the correspondence of the theory with the experiments is surprisingly good in the quantitative sense.

Analysing the problem it has been demonstrated that the space charge effect of the axial component of the electric field can be transformed into a variable effective length of the electron beam. For practical purpose the knowledge of the effective

38

length and of the parameters on which it depends is of great importance as it makes it possible to find the optimal performance of the omegatron for a given purpose. It is e.g. well-known from experiments that hydrogen can be registered by the omegatron only with difficulties. This experience can be explained easily with the aid of effective length. Under conditions favorable for most common gases, hydrogen has a too high value of $\varkappa$ and consequently the corresponding effective length is very low.

References

[1] Urgošík B., Elektrotech. čas., 30 1979 20.
[2] Vejvodová J., Urbánková H., Acta Univ. Carol., Math. Phys., 18 1977, 3.
[3] Zinčenko N. S., Kurs po elektronnoj optike, Izd. Gos. Univ. Charkov, 1961.
[4] Berry C. E., J. Appl. Phys., 25 1954, 28.
[5] Klopfer A., Schmidt W., Vac. 10 1960, 363.
[6] Urgošík B., Čs. Čas. Fys., 14 1964, 163.